Supporting Information

For

Involvement of a Formally Cu(III) Nitrite Complex in PCET and Nitration of Phenols

Caitlin J. Bouchey[a,b] and William B. Tolman[a,*]

[a]Department of Chemistry, Washington University in St. Louis, One Brookings Drive, Campus Box 1134, St. Louis, Missouri 63130, United States

[b]Department of Chemistry, University of Minnesota, 207 Pleasant Street SE, Minneapolis, Minnesota 55455, United States

* Corresponding author: wbtolman@wustl.edu

Table of Contents

1. Experimental materials and methods.

General comments. Metal complexes were synthesized and handled under a dinitrogen atmosphere in a Vacuum Atmospheres glovebox or an argon atmosphere using Schlenk techniques. All reagents and solvents were purchased from commercial sources unless otherwise noted. Tetrahydrofuran, acetonitrile, diethyl ether, dichloromethane, and pentane were passed through activated alumina columns and plumbed directly into a glovebox. Tetrahydrofuran and dichloromethane were stored over activated 3 Å molecular sieves in a dinitrogen-filled glovebox and, prior to use in spectroscopy and cyclic voltammetry experiments, filtered using a 25 mm diameter, 0.2 mm hydrophobic polytetrafluoroethylene (PTFE) syringe filter. Dry acetone was purchased from Sigma-Aldrich and used without purification. 2,4,6-tri-*t*-butylphenol (TTBP) and 2,4-di-*t*-butylphenol (DTBP) were recrystallized several times from saturated pentane solutions at -30 ˚C prior to use. LCu(MeCN)[1] and acetyl ferrocenium tetrakis(3,5-bis(trifluoromethyl)phenyl)borate ([AcFc][$BArF_{24}$])[2] were synthesized according to the published procedures. Bis(triphenylphosphine)iminium chloride (PPNCl), $AgNO_2$, [NBu_4][NO_2], Fc*, Fc, [NO][SbF_6], and trimethoxybenzene were purchased from Sigma-Aldrich and CoTPP was purchased from Strem Chemicals, and all were used without further purification.

UV-vis spectra were collected on a HP8453 (190-1100 nm) diode array spectrophotometer equipped with a Unisoku low-temperature UV-vis cell holder. EPR data were collected on frozen 1 mM samples with a CW Elexsys E500 EPR spectrometer using X-band (9.38 GHz) radiation at 35 dB and at 30 K. The microwave power, modulation amplitude, and modulation frequency were 0.0002 mW, 9.8 G, and 100 kHz, respectively. EPR spectral simulations were performed using the EasySpin EPR simulation package, v. 5.1, in Matlab.[3] NMR spectra were collected on a Varian Unity Inova (500 MHz) spectrometer. Deuterated chloroform ($CDCl_3$) was purchased from

Cambridge Isotopes Laboratories, degassed, and dried over 3 Å molecular sieves prior to use. Cyclic voltammograms were recorded using an EC Epsilon potentiostat from BASi, a glassy carbon working electrode, a Pt counter electrode, and a Ag wire pseudoreference electrode. All cyclic voltammograms were performed in THF with 0.3 M tetrabutylammonium hexafluorophosphate (TBAP) electrolyte, which was recrystallized several times from ethanol and dried under high-vacuum before use, and were internally referenced to the ferrocene/ferrocenium (Fc/Fc^+) couple. The spectra were converted vs. the standard Fc/Fc^+ couple using standard conversion factors.[4] Elemental Analysis was performed by the CENTC Elemental Analysis Facility (University of Rochester).

For X-ray crystallography experiments, crystals were placed onto the tip of a MiTeGen cryoloop and mounted on a Bruker D8 VENTURE diffactometer equipped with a Photon III CMOS. The data collections were carried out using Mo Kα source using normal parabolic mirrors as monochromators at 173 K. Structure solutions were performed with SHELXT[5] using ShelXle[6] as a graphical interface. The structures were refined against F^2 on all data by full-matrix-least-squares with SHELXL.[7] The CCSD deposition number is: 2125948.

Resonance Raman spectra were obtained by collecting the collimated Raman scattering using a Plano convex lens (f = 10 cm, placed at an appropriate distance) through appropriate long-pass edge filter (Semrock). The spectra were collected by an Andor Shamrock 500i monochromator (SR-500I-A) with an Andor Newton 920 thermo-electric cooled CCD detector (DU920P-BU), which was cooled to -90 °C before collection. Data collection was interfaced with Andor Solis (s) software. Spectral data was collected on frozen samples at 77 K in EPR tubes using 135° backscattering geometry. Excitation at 660 nm was provided by a Cobolt Flamenco 660 nm 100 mW laser. Raman shifts were externally referenced to indene and internally referenced to

solvent. Each spectrum was an accumulation of 450 spectra with 4 s acquisition times, resulting in 30 min collections. All spectra were baseline corrected using a multi-point correction within the software Spectragryph.[8]

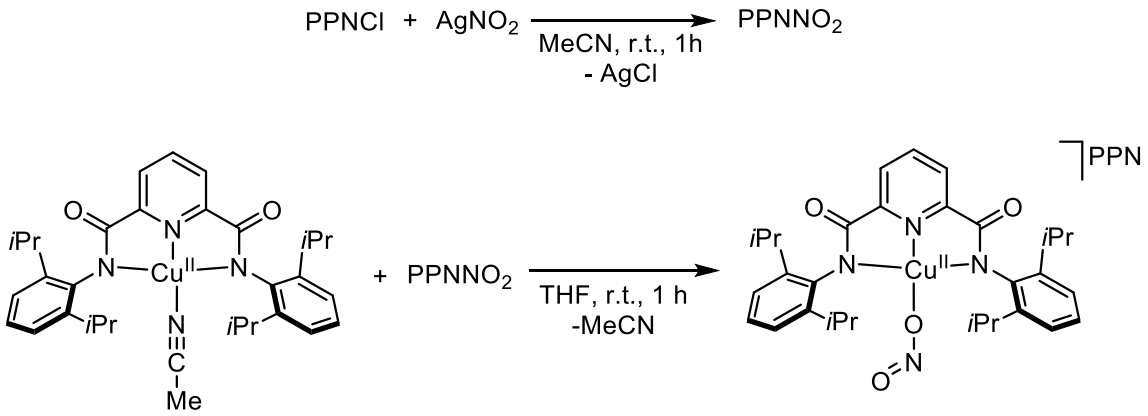

Synthesis of [PPN][LCuNO$_2$]. A solution of PPNCl (1.696 g, 2.95 mmol) in anhydrous acetonitrile (5 mL) was added to 20 mL scintillation vial, covered in aluminum foil, containing $AgNO_2$ (0.500 g, 3.25 mmol) and acetonitrile (5 mL) and stirred for 1 h. The solvent was removed *in vacuo* and the pale orange, oily solid was dissolved in dry acetone (12 mL). Dry diethyl ether (8 mL) was slowly added down the side of the vial while crystals began to form. The vial was capped and stored at -30 °C overnight. The next day, the crystals were filtered, isolated, and residual solvents were removed *in vacuo*. After 1 week, the batch of crystals appeared to contain some silver decomposition products, so the batch was dissolved in DCM, filtered through a 25 mm diameter, 0.2 mm hydrophobic polytetrafluoroethylene (PTFE) syringe filter. LCuMeCN (50.0 mg, 0.085 mmol) was dissolved in THF (3 mL) in a 20 mL scintillation vial. To this vial, a slurry of [PPN][NO_2] (49.7 mg, 0.085 mmol) in THF (3 x 2 mL) was added quantitatively. After stirring for 1 h, the solution turned navy blue, and the solvent was removed *in vacuo*. The blue oil was triturated with pentane (2 x 5 mL) and the solvent was decanted and the resulting blue powder was dried *in vacuo* (83.5 mg, 87%). X-ray quality crystals were grown by dissolving the product in

THF (1 mL) and using diethyl ether for vapor diffusion at room temperature over 3 days (navy blue/gray plates). UV-vis (THF, X °C) λ_{max}, nm (ε, M^{-1} cm^{-1}): 311 (8288), 385 (2509), 586 (454). Anal. calcd (%) for $C_{67}H_{67}CuN_5O_4P_2$: C, 71.10; H, 5.97; N, 6.19. Found: C, 70.73; H, 5.91; N, 5.91.

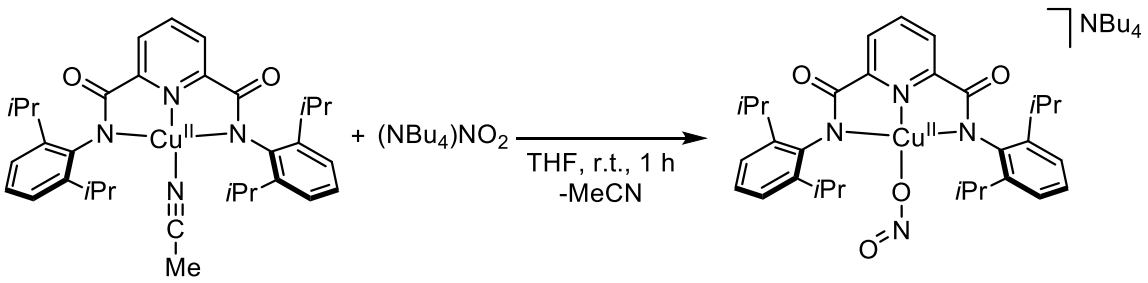

Synthesis of [NBu$_4$][LCuNO$_2$]. LCuMeCN (200.0 mg, 0.340 mmol) was dissolved in THF (4 mL) in a 20 mL scintillation vial. To this vial, a solution of [NBu$_4$][NO$_2$] (98.1 mg, 0.340 mmol) in THF (3 x 2 mL) was added quantitatively. After stirring for 1 h, the solution turned navy blue and the solvent was removed *in vacuo*. The oily product was triturated with pentane (2 x 5 mL) and the solvent was decanted then further removed *in vacuo* yielding a powder blue powder (253.0 mg, 89%). UV-vis (THF, -80 °C) λ_{max}, nm (ε, M^{-1} cm^{-1}): 311 (8594), 385 (2614), 586 (470). Anal. calcd (%) for $C_{47}H_{75}CuN_5O_5$ (as [NBu4][LCuNO2] • H_2O): C, 66.13; H, 8.86; N, 8.20. Found: C, 66.58; H, 8.57; N, 8.08.

2. EPR spectral data for complexes [NBu4][LCuNO2] and [PPN][LCuNO2]

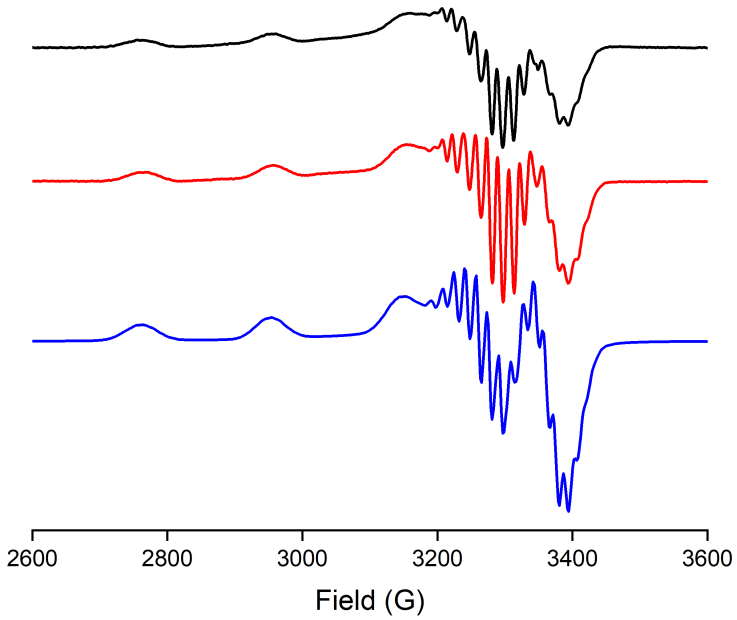

Figure S1. Continuous wave X-band (9.38 GHz) EPR spectrum of 1 mM [NBu4][LCuNO2] in THF at 30 K (black), 1 mM [PPN][LCuNO2] in THF at 30 K (red), and the simulation of $[LCuNO2]^-$ (blue).

Table S1. Simulated g-values and hyperfine/superhyperfine parameters (MHz) for Cu, $N^{pyridine}$, and N^{amide} nuclei for [PPN][LCuNO2] in THF at 30 K.

[PPN][LCuNO2]											
g_x	g_y	g_z	$A^{Cu}{}_x$	$A^{Cu}{}_y$	$A^{Cu}{}_z$	$A^{py}{}_x$	$A^{py}{}_x$	$A^{py}{}_z$	$A^{am}{}_x$	$A^{am}{}_y$	$A^{am}{}_z$
2.09	2.11	2.26	55	60	595	33	50	40	48	50	40

3. UV-vis spectral data for complexes [NBu_4][$LCuNO_2$] and [PPN][$LCuNO_2$]

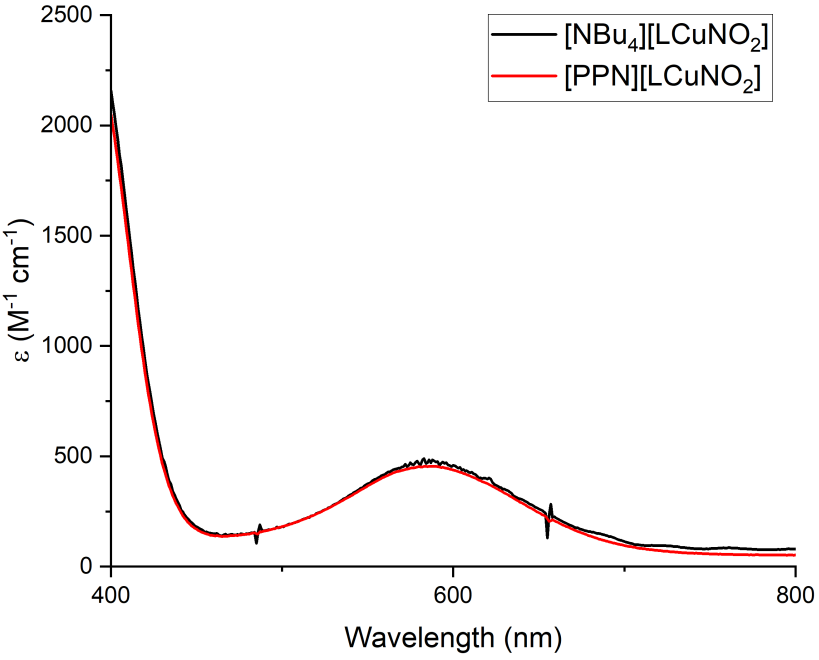

Figure S2. Overlay of the UV-vis spectra of [NBu_4][$LCuNO_2$] (black) and [PPN][$LCuNO_2$] (red) in THF at -80 ˚C.

4. Cyclic votammogram data

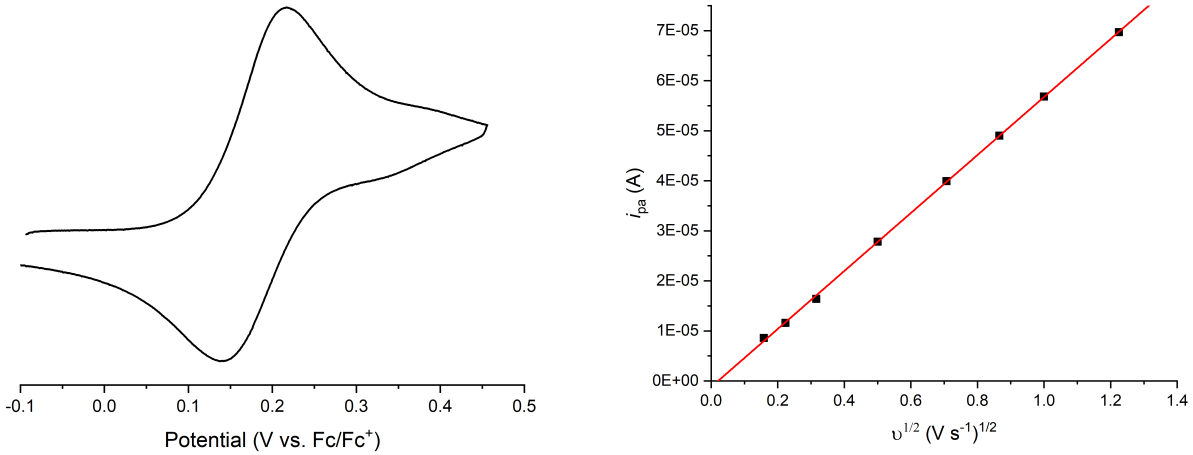

Figure S3. (Left) Cyclic voltammogram collected of [NBu_4][$LCuNO_2$]. Conditions: 2 mM [$LCuNO_2$], 0.3 M TBAP, THF, 25 °C, glassy-carbon working electrode, 100 mV/s scan rate. (Right) Anodic current response as a function of the square root of the scan rate.

Table S2. Cyclic voltammetry data for $[LCuX]^{-/0}$ [a]

Complex	$E_{1/2}$ (mV)[b]	Ref.
$[LCuSPh]^-$	-251	[9]
$[LCuSH]^-$	-209	[9]
$[LCuOOtBu]^-$	-205	[10]
$[LCuOH]^-$	-167	[11]
$[LCuOOCMe_2Ph]^-$	-154	[10]
$[LCuOCH_2CF_3]^-$	37	[12]
$[LCuO_2CCH_3]^-$	150	[12]
$[LCuO_2CC_6H_4(OMe)]^-$	151	[12]
$[LCuO_2CC_6H_5]^-$	169	[12]
$[LCuNO_2]^-$	180	this work
$[LCuO_2CC_6H_4(Cl)]^-$	228	[12,13]
$[LCuO_2CC_6H_4(NO_2)]^-$	239	[12]
$[LCuO_2CC_6F_5]^-$	298	[12]

5. Oxidation of Cu^{II}

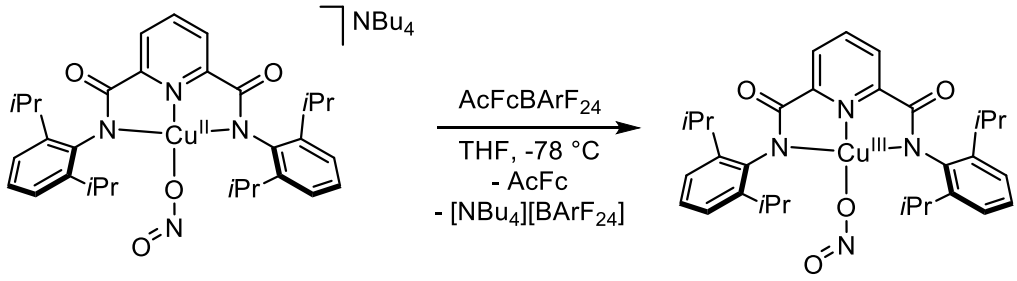

General procedure for the generation of $LCuNO_2$. A solution of $[NBu_4][LCuNO_2]$ in THF (0.2 mL, 2 mM) was injected into a UV-vis cuvette under Ar containing THF (1.6 mL) at -80 °C, set by the Unisoku low temperature UV-vis cell holder. After stirring and temperature equilibration (5 min), a UV-vis spectrum was recorded. With stirring, a solution of $[AcFc][BArF_{24}]$ in THF (0.1 mL, 4 mM) was added to the cuvette (final concentration of 0.2 mM) and a spectrum was immediately recorded. For titration experiments, solution of $[NBu_4][LCuNO_2]$ in THF (0.2 mL, 2 mM) was injected into a UV-vis cuvette under Ar containing THF (1.3 mL) at -80 °C, set by the Unisoku low temperature UV-vis cell holder. After stirring and temperature equilibration (5 min), a UV-vis spectrum was recorded. With stirring, aliquots of an $[AcFc][BArF_{24}]$ solution in THF (0.8 mM) were added in 0.1 mL increments (0.2 eq.), up to 1.8 eq., to the cuvette and a spectrum

was immediately recorded after each injection. A resonance Raman sample was prepared by cooling an EPR tube under Ar containing a solution of [NBu4][$LCuNO_2$] in THF (0.4 mL, 4 or 8 mM) and a stir bar to -78 °C in an acetone/dry ice-cold bath. A solution of [AcFc][$BArF_{24}$] in THF (0.4 mL, 4 or 8 mM) was slowly added down the side of the EPR tube and a magnetic stir bar retriever was submerged into the cold bath and used to thoroughly mix the contents of EPR tube. In rapid succession, the Ar supply and stir bar were removed, the outside of the EPR tube was wiped free of acetone and the tube was dunked into liquid nitrogen to freeze the sample.

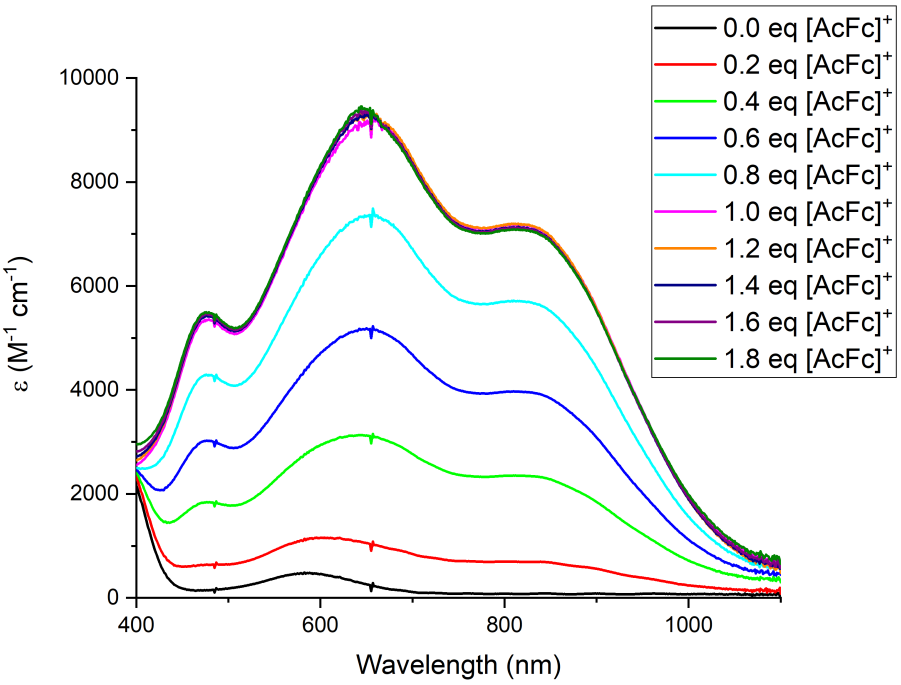

Figure S4. Overlay of UV-vis spectra upon addition of incremental equivalents of [AcFc][$BArF_{24}$] to [NBu_4][$LCuNO_2$] at -80 °C in THF.

6. Chemical reversibility of $LCuNO_2^{0/-}$

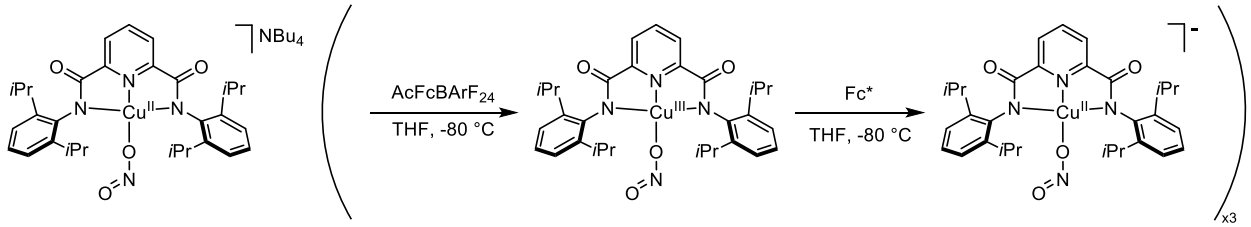

General procedure for the reversible oxidation/reduction of [NBu₄][LCuNO₂]. A solution of [NBu4][LCuNO2] in THF (0.2 mL, 2 mM) was injected into a UV-vis cuvette under Ar containing THF (1.7 mL) at -80 °C, set by the Unisoku low temperature UV-vis cell holder. After stirring and temperature equilibration (5 min), a UV-vis spectrum was recorded. With stirring, a solution of [AcFc][BArF24] in THF (0.1 mL, 4 mM) was added to the cuvette and a spectrum was immediately recorded. An aliquot of a Fc* solution in THF (0.1 mL, 4 mM) was added to the cuvette with stirring and another spectrum was immediately recorded. The chemical oxidation and reduction processes were repeated twice more, and spectra were recorded after each addition of reagent.

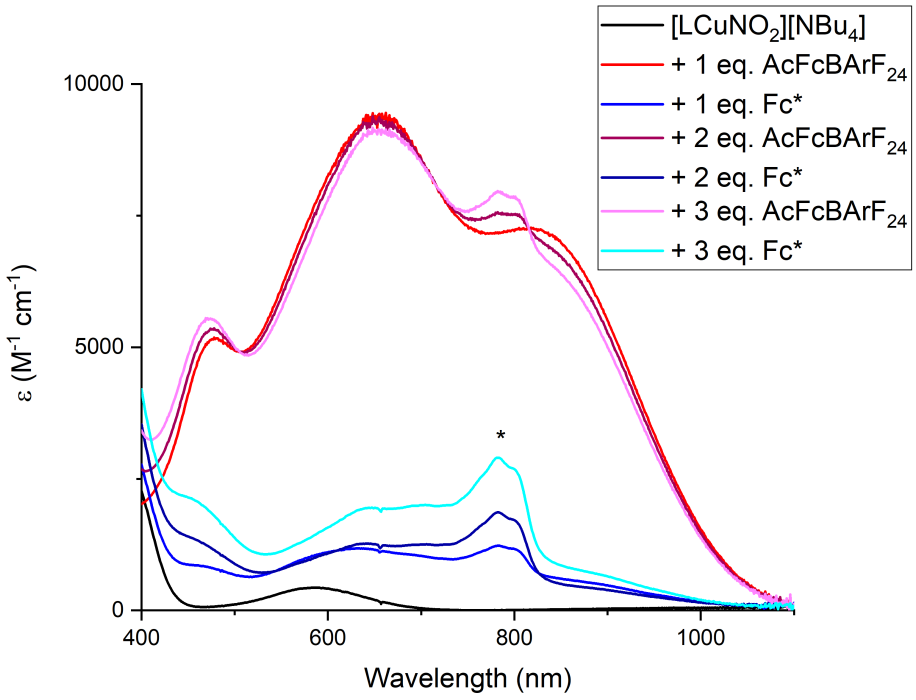

Figure S5. UV-vis chemical oxidation/reduction titration where up to 3 eq. of [AcFc][BArF24] and Fc* were added to [NBu4][LCuNO2] in THF at -80 °C (*denotes Fc^{*+} signal).

7. Resonance Raman spectroscopy of $LCuNO_2$

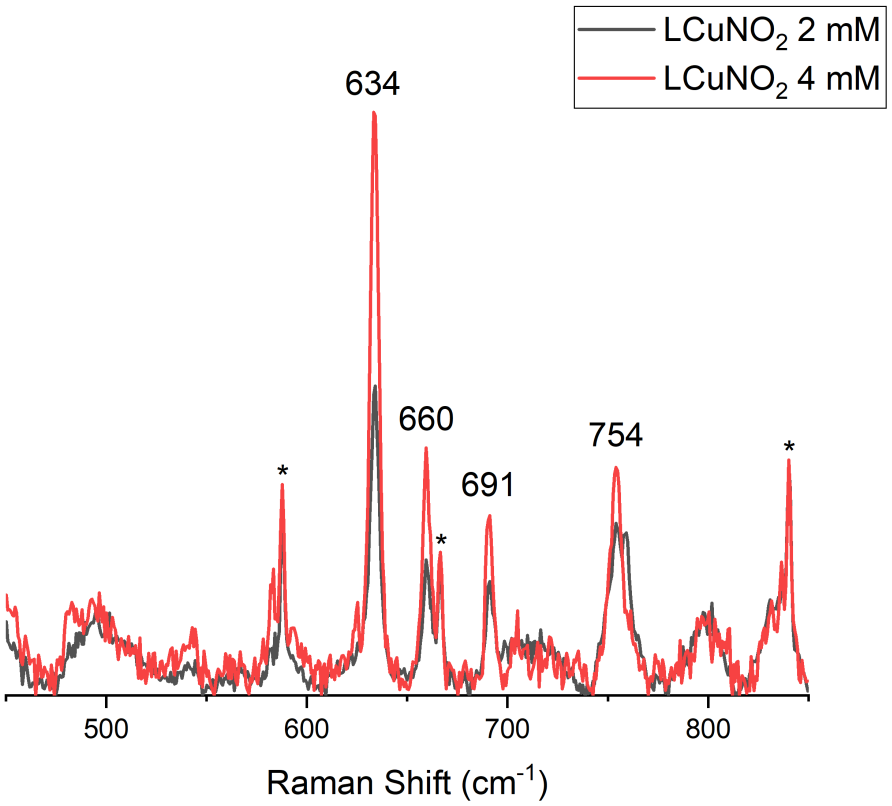

Figure S6. Resonance Raman spectra (λ_{ex} = 660 nm) of frozen $LCuNO_2$ samples in THF (2 mM, black and 4 mM, red). Peaks with concentration dependence are labelled. (* denotes solvent)

8. Reactivity of $LCuNO_2$ with phenols

General procedure for the reactions between $LCuNO_2$ and phenol. A UV-vis cuvette under Ar containing THF (1.6 mL) at -80 °C (TTBP) or -40 °C (DTBP), set by the Unisoku low temperature UV-vis cell holder, was charged with a THF solution of $[LCuNO_2][NBu_4]$ (0.2 mL, 2mM). The solution was allowed to cool (5 min) with stirring and a continuous collection of spectra was initiated. Quickly after, a THF solution of $[AcFc][BArF_{24}]$ (0.1 mL, 4 mM) was injected into the cuvette. When the new features were fully formed, a THF solution of phenol (0.1 mL, various eq.) was quickly added, and the decay was observed until no further changes were observed. The k_2 values for the reactions between $LCuNO_2$ and TTBP (50 eq.) were calculated by using ReactLab Kinetics[14] using the known concentrations. EPR product analysis and

quantification of the phenoxyl radical from the reaction between $LCuNO_2$ and TTBP were carried out by adding THF (0.3 mL) and a THF solution of $[LCuNO_2][NBu_4]$ (0.1 mL, 0.6 mM) to an EPR tube containing a stir bar in the glovebox. The EPR tube was sealed with a septum cap, removed from the glovebox, and put under Ar on a Schlenk line. The tube was cooled to -78 °C in an acetone/dry ice-cold bath for 15 min when a THF solution of $[AcFc][BArF_{24}]$ (0.1 mL, 0.6 mM) was slowly added down the side of the tube. A magnetic stir bar retriever was dunked into the cold bath and used to mix the solution. A THF solution of TTBP (0.1 mL, 30 mM, 50 eq.) was then slowly added down the side of the tube and the magnetic stir bar retriever was once again used to mix the solution. The reaction was allowed to proceed for 15 mins then frozen by, in rapid succession, removing the Ar flow, septum cap, and magnetic stir bar, wiping off the acetone from the outside of the tube, and dunking the tube into liquid nitrogen. The yield of the phenoxyl radical was calculated by finding the relative intensities of the double integration spectra for the reaction (0.1 mM in Cu, 5 mM in TTBP), TEMPO· (0.1 mM), and $[PPN][LCuNO_2]$ (1 mM) and using them in the following equation: [(intensity of reaction spectrum - spectrum - [intensity of $[PPN][LCuNO_2]$ spectrum/10])/(intensity of TEMPO·)]*100. The yield of NO released from the reaction between $LCuNO_2$ and TTBP (50 eq.) was found by placing a 1-dram vial inside a 20 mL vial that could be equipped with a cap containing a pierceable septum. THF (1.6 mL) was added to the inner 1-dram vial and a DCM solution of CoTPP (0.2 mM, 2 mL) was added to the outer vial. The 2-vial setup and THF solutions of $[NBu_4][LCuNO_2]$, $[AcFc][BArF_{24}]$, and TTBP were cooled to -40 °C in a cold-well using an acetonitrile/dry ice-cold bath for 15 min. At -40 °C, the THF solutions of $[NBu_4][LCuNO_2]$ (2 mM, 0.2 mL) and $[AcFc][BArF_{24}]$ (4 mM, 0.1 mL) were syringed into the inner 1-dram vial to generate $LCuNO_2$. The 2-vial setup was capped with a pierceable septum cap and the THF solution of TTBP (50 eq., 200 mM, 0.1 mL) was spiked into

the inner 1-dram vial. The reaction setup was allowed to come to room temperature for 1 h. An aliquot of the DCM solution of CoTPP in the outer vial was diluted with DCM (final concentration of 5 μM) and a room temperature UV-vis spectrum was recorded. The resulting spectrum was compared to pure CoTPP and (NO)CoTPP, which was generated via the same 2-vial setup using Fc and [NO][SbF_6] (50 eq.) in the inner 1-dram vial, using the Gaussian fitting function in Origin 2021b. The reactions between $LCuNO_2$ and various equivalents of DTBP (1 – 60 eq.) were analyzed using the natural log of the absorbance at a single wavelength (655 nm) over time. These plots were fit to a linear decay to attempt to derive pseudo-first order k_{obs} values for the various equivalents. The fits were found to be inappropriate because the data deviates from linearity due to more complicated kinetics occurring.

8.1. UV-vis decay spectra of the reaction between $LCuNO_2$ and TTBP

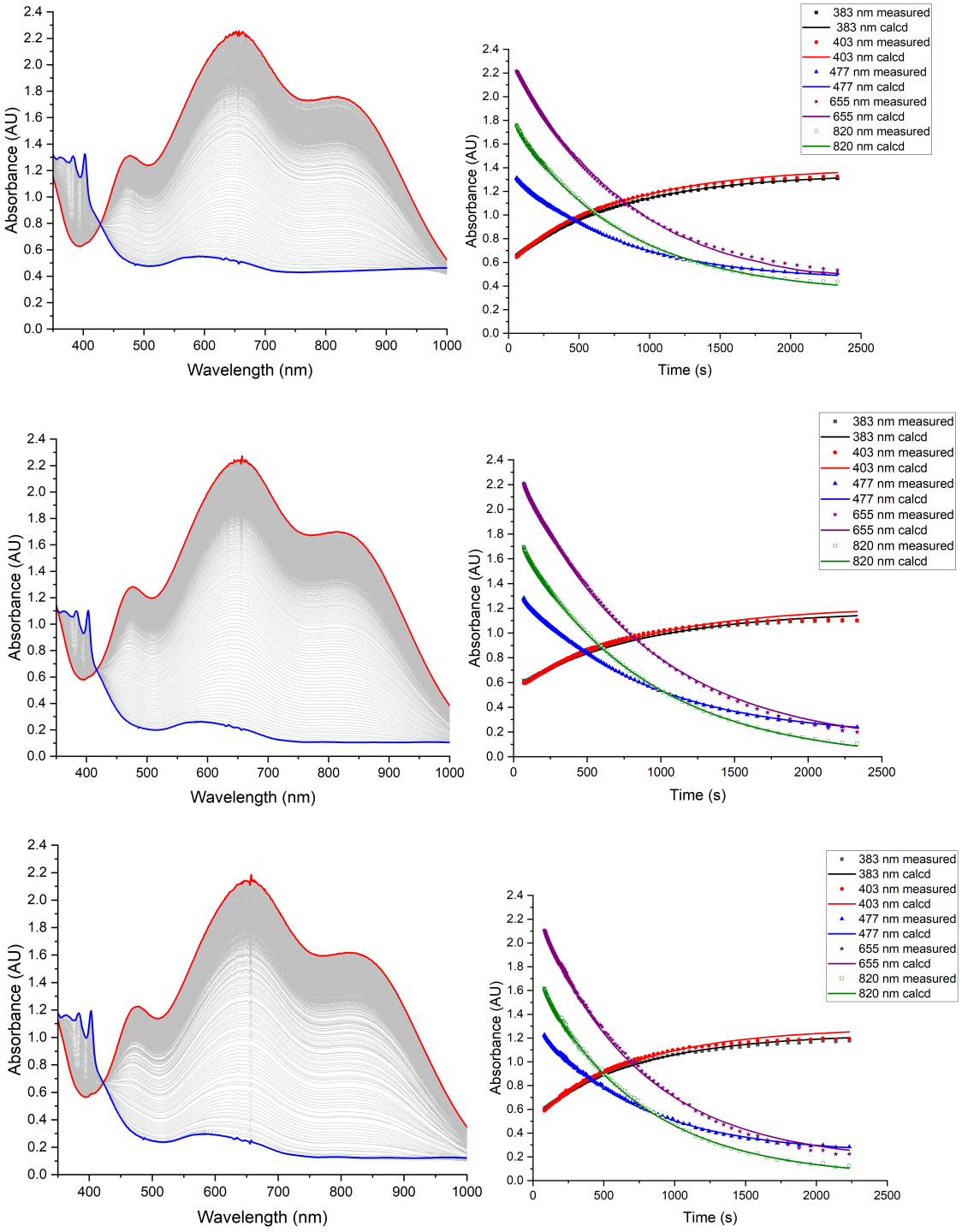

Figure S7. (Left column) Triplicate UV-vis spectra as a function of time for the reactions of $LCuNO_2$ (red) with TTBP (50 eq.) in THF at -80 °C. The product spectrum (blue) is assigned as LCuTHF and the phenoxyl radical of TTBP. (Right column) Plots of absorbance vs. time at representative wavelengths (λ = 383, 403, 477, 655 and 820 nm) for the respective decay plots in the right column. The plots contain an overlay of experimental (scatter plots) and calculated (lines) data to represent the accuracy of the fit from ReactLab Kinetics, which was used to calculate the k_2 value discussed in the manuscript.

8.2. Product analysis of the reaction between $LCuNO_2$ and TTBP

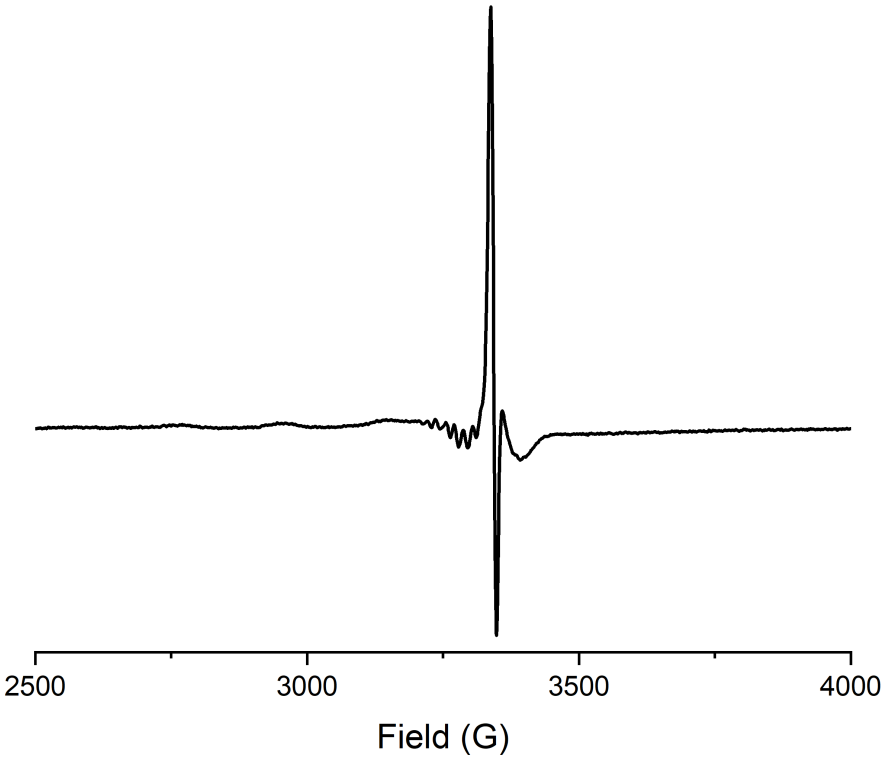

Figure S8. Continuous wave X-band (9.38 GHz) EPR spectrum of the products of the reaction between 0.1 mM $LCuNO_2$ and 50 eq. of TTBP in THF at 30 K.

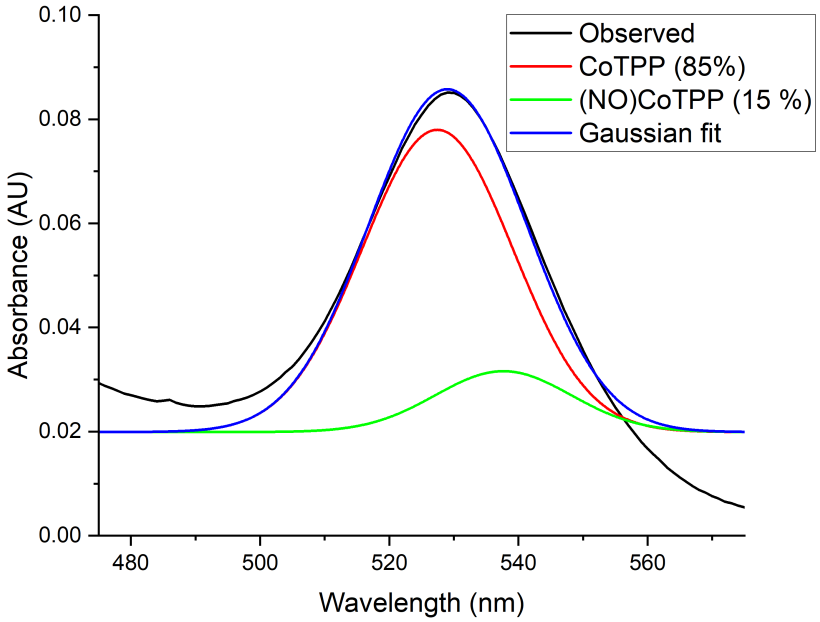

Figure S9. UV-vis spectrum and Gaussian fits of the DCM solution containing CoTPP after exposure to the headspace of the reaction between $LCuNO_2$ and TTBP.

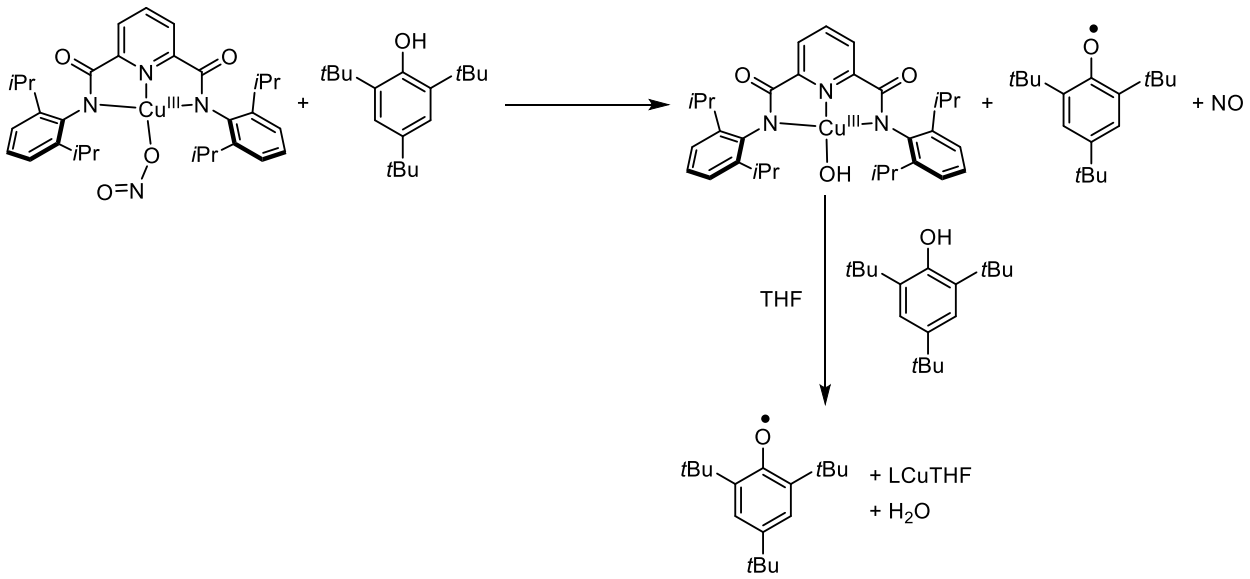

Scheme S1. An alternative mechanism of the PCET reaction of $LCuNO_2$ and TTBP where $LCuNO_2$ abstracts an H-atom from TTBP resulting in O–N bond cleavage to give products LCuOH, the phenoxyl radical, and NO. LCuOH is known to quickly react with TTBP so this mechanism would result in two eq. of the phenoxyl radical product in the presence of excess TTBP.

8.3. Plot of $E_{1/2}$ $LCuX^{0/-}$ vs. log(k_2) of the reaction between LCuX and TTBP

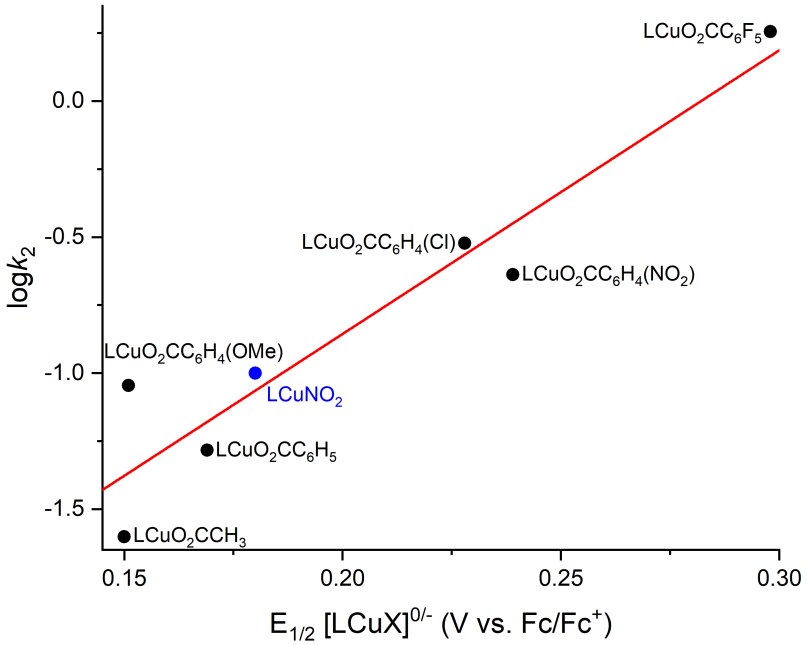

Figure S10. Plot of $E_{1/2}$ for the $[LCuX]^{0/-}$ couple in THF vs the log k_2 values for the reactions between LCuX and TTBP at -80 ˚C in THF. Figure reproduced from reference 12.

8.4. UV-vis decay spectra of the reactions between $LCuNO_2$ and various equivalents of DTBP

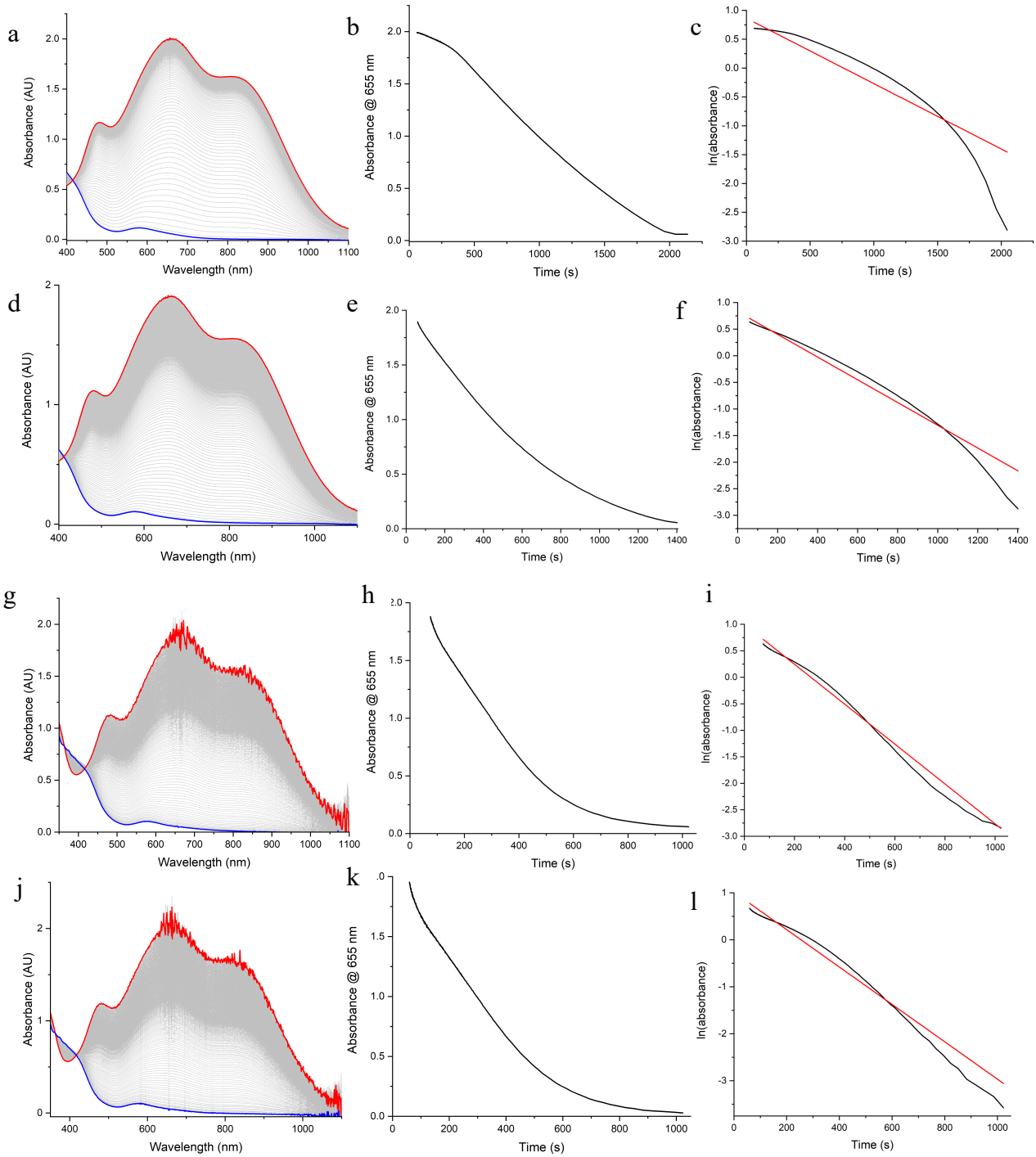

Figure S11. (a, d, g, j) UV-vis spectra as a function of time for the reaction between $LCuNO_2$ (red) and DTBP (a, d, g, j: 1 eq., 20 eq. 40 eq. 60 eq.) in THF at -40 °C. The product spectrum (blue) is assigned as LCuTHF. (b, e, h, k) Plot of absorbance vs. time at 655 nm for the reaction between $LCuNO_2$ and DTBP in THF at -40 °C (b, e, h, k: 1 eq., 20 eq. 40 eq. 60 eq.: $t_{1/2}$ = 613, 318, 252, 176 s). (c, f, i, l) Plot of ln(absorbance) vs. time at 655 nm (black) and a linear fit (red) for the reaction between LCuNO2 and DTBP (c, f, i, l: 1 eq., 20 eq. 40 eq. 60 eq.) in THF at -40 °C.

9. Organic product analysis of the reactions between $LCuNO_2$ and various equivalents of DTBP

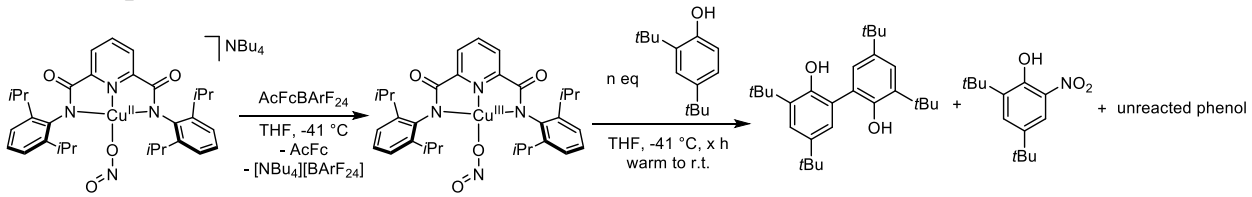

General procedure for organic product analysis of the reactions between $LCuNO_2$ and DTBP. THF solutions of $[NBu_4][LCuNO_2]$, $[AcFc][BArF_{24}]$, DTBP, a clean 20 mL scintillation vial were cooled for 10 minutes in a -41 °C coldwell generated by an acetonitrile/dry ice bath. The 20 mL scintillation vial was charged with the THF solution of $[NBu_4][LCuNO_2]$ (8 mM, 1 mL) followed by the THF solution of $[AcFc][BArF_{24}]$ (8 mM, 1 mL) to generate $LCuNO_2$. Then, the THF solution of DTBP (80 mM, 1 mL for 10 eq.; 8 mM, 1 mL for 1 eq.; 4 mM, 1 mL for 0.5 eq.) was immediately injected into the vial and the reaction was allowed to proceed in the coldwell for an allotted time (1 h when 10 eq. employed; 2 h when either 1 eq. or 0.5 eq. employed). The reaction mixture was brought to room temperature when the solvent was removed *in vacuo*. The residue was dissolved in DCM (1 mL) and the solution was run through a 3-inch silica plug in a pipette. The vial and plug were rinsed with DCM (2 x 1 mL). A THF solution of trimethoxybenzene (8 mM, 1 mL) was added to the resulting DCM solution and the solvent was removed *in vacuo*. The residue was dissolved in $CDCl_3$ (1 mL) and a quantitative ^1H NMR spectrum was obtained.

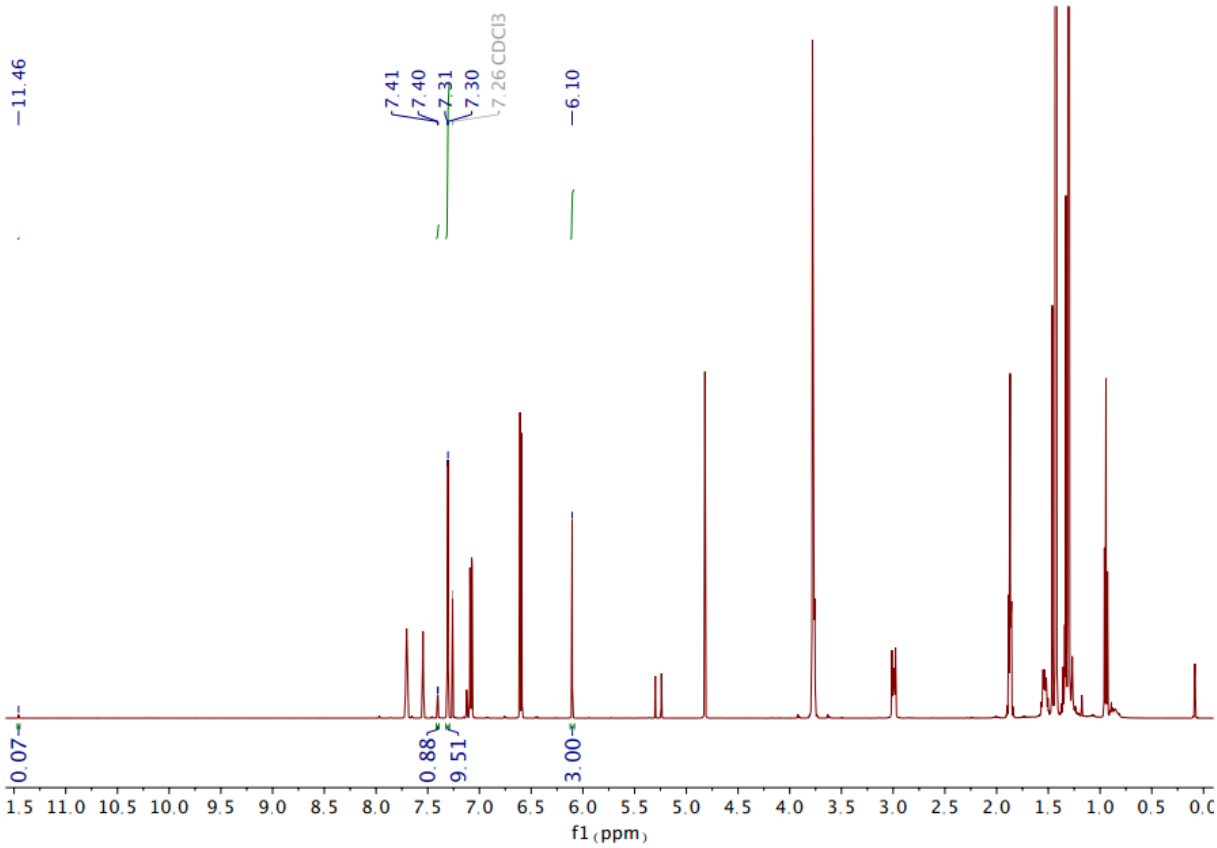

Figure S12. Representative ^{1}H NMR of the products from the reaction between $LCuNO_2$ and 10 eq. of DTBP.

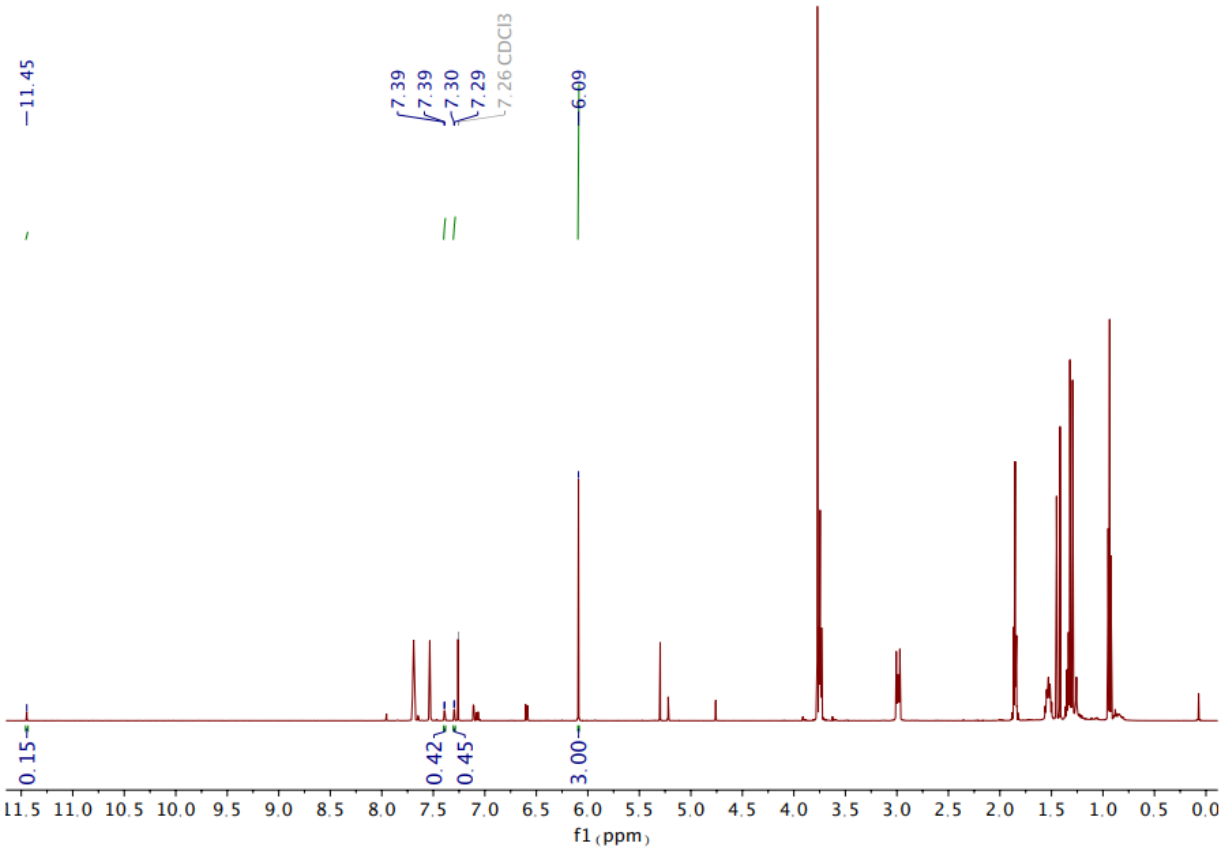

Figure S13. Representative ^{1}H NMR of the products from the reaction between $LCuNO_2$ and 1 eq. of DTBP.

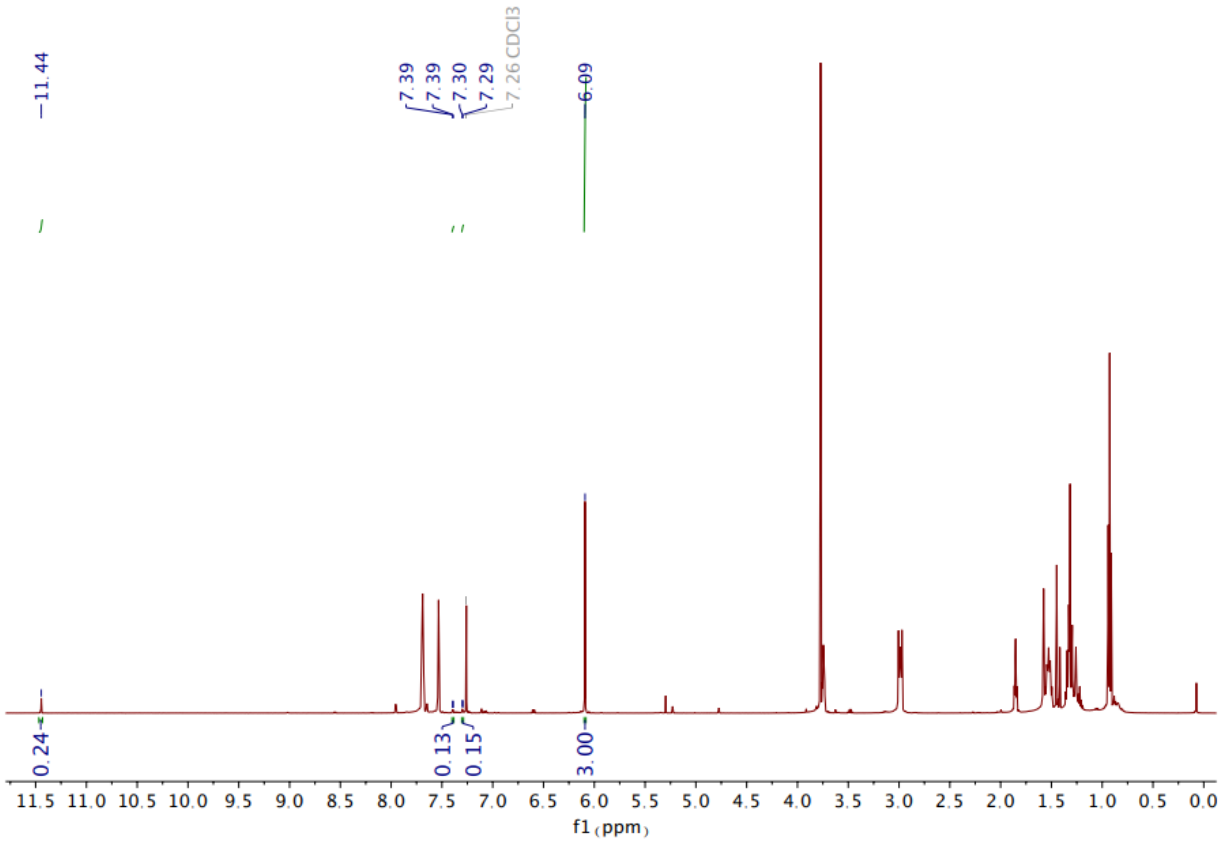

Figure S14. Representative ^{1}H NMR of the products from the reaction between $LCuNO_2$ and 0.5 eq. of DTBP.

10. Alternative phenol nitration mechanism

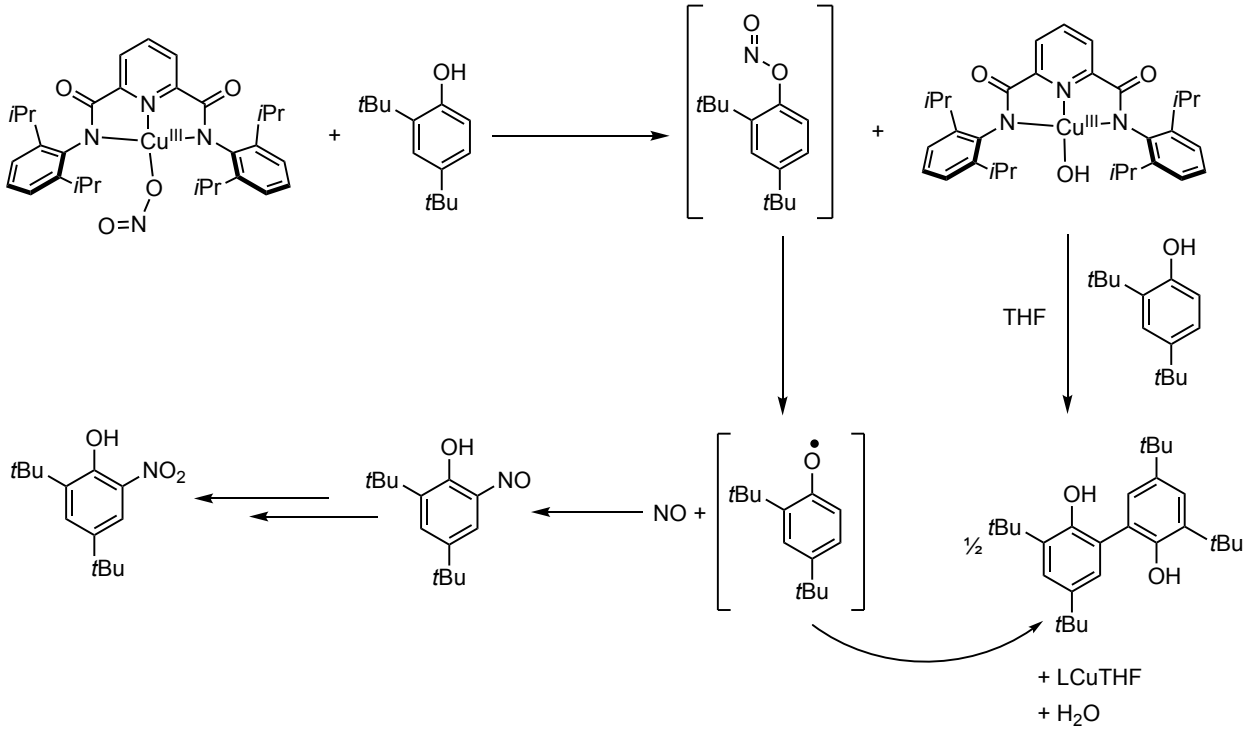

Scheme S2. An alternative mechanism for nitration of DTBP by $LCuNO_2$ involving nucleophilic attack of the phenol on the nitrite ligand of $LCuNO_2$.

11. References

[1] Donoghue, P. J.; Gupta, A. K.; Boyce, D. W.; Cramer, C. J.; Tolman, W. B. An Anionic , Tetragonal Copper(II) Superoxide Complex. *J. Am. Chem. Soc.* **2010**, *132* (45), 15869–15871.

[2] Dhar, D.; Yee, G. M.; Spaeth, A. D.; Boyce, D. W.; Zhang, H.; Dereli, B.; Cramer, C. J.; Tolman, W. B. Perturbing the Copper(III)-Hydroxide Unit through Ligand Structural Variation. *J. Am. Chem. Soc.* **2016**, *138* (1), 356–368.

[3] Stoll, S.; Schweiger, A. EasySpin, a comprehensive software package for spectral simulation and analysis in EPR. *J. Magn. Reson.* **2006**, *178* (1), 42-55.

[4] Noviandri, I.; Brownm K. N.; Fleming, D. S.; Gulyas, P. T.; Lay, P. A.; Masters, A. F.; Phillips, L. The Decamethylferrocenium/Decamethylferrocene Redox Couple: A Superior Redox Standard to the Ferrocenium/Ferrocene Redox Couple for Studying Solvent Effects on the Thermodynamics of Electron Transfer. *J. Phys. Chem. B* **1999**, *103* (32), 6713-6722.

[5] Sheldrick, G. M., "SHELXT – Integrated space-group and crystal structure determination," *Acta. Cryst.* **2015**, *A71*, 3-8.

[6] Hubschle, C. B.; Sheldrick, G. M.; Dittrich, B., "ShelXle: a Qt graphical interface for SHELXL," *J. Appl. Cryst.* **2011**, *44*, 1281-1284.

[7] Sheldrick, G. M., "A short history of SHELX," *Acta. Cryst.* **2008**, *A64*, 112-122.

[8] Menges, F. Spectragryph – optical spectroscopy software, Version 1.2.14, **2020**, http://www.effemm2.de/spectragryph/

[9] Wu, W.; Tehranchi De Hont, J.; Vlaisavljevich, B.; Tolman, W. B. Sulfur-Containing Analogues of the Reactive [CuOH]2+ Core. *Inorg. Chem.* **2021**, *60* (7), 5217–5223.

[10] Neisen, B. D.; Gagnon, N. L.; Dhar, D.; Spaeth, A. D.; Tolman, W. B. Formally Copper(III)-Alkylperoxo Complexes as Models of Possible Intermediates in Monooxygenase Enzymes. *J. Am. Chem. Soc.* **2017**, *139* (30), 10220–10223.

[11] Krishnan, V. M.; Shopov, D. Y.; Bouchey, C. J.; Bailey, W. D.; Parveen, R.; Vlaisavljevich, B.; Tolman, W. B. Structural Characterization of the [CuOR]2+Core. *J. Am. Chem. Soc.* **2021**, *143* (9), 3295–3299.

[12] Elwell, C. E.; Mandal, M.; Bouchey, C. J.; Que, L.; Cramer, C. J.; Tolman, W. B. Carboxylate Structural Effects on the Properties and Proton-Coupled Electron Transfer Reactivity of [CuO2CR]2+ Cores. *Inorg. Chem.* **2019**, *58* (23), 15872.

[13] Mandal, M.; Elwell, C. E.; Bouchey, C. J.; Zerk, T. J.; Tolman, W. B.; Cramer, C. J. Mechanisms for Hydrogen-Atom Abstraction by Mononuclear Copper(III) Cores: Hydrogen-Atom Transfer or Concerted Proton-Coupled Electron Transfer? *J. Am. Chem. Soc.* **2019**, *141* (43), 17236.

[14] Maeder, M.; King, P. Reactlab, Jplus Consulting Pty Ltd: East Freemantle, WA. Australia, 2009.